Liquid Crystals
Publication details, including instructions for authors and subscription information:
http://www.informaworld.com/smpp/title~content=t713926090

X-ray diffraction study of the smectic A phases of some side-chain polysiloxanes

P. Davidson[a]; A. M. Levelut[a]; M. F. Achard[b]; F. Hardouin[b]
[a] Laboratoire de Physique des Solides associé au CNRS Bat. 510, Université Paris XI, Orsay Cedex, France [b] Centre de Recherche Paul Pascal, Université de Bordeaux I, Talence, France

To cite this Article Davidson, P. , Levelut, A. M. , Achard, M. F. and Hardouin, F.(1989) 'X-ray diffraction study of the smectic A phases of some side-chain polysiloxanes', Liquid Crystals, 4: 5, 561 — 571
To link to this Article: DOI: 10.1080/02678298908033191
URL: http://dx.doi.org/10.1080/02678298908033191

LIQUID CRYSTALS, 1989, VOL. 4, NO. 5, 561–571

X-ray diffraction study of the smectic A phases of some side-chain polysiloxanes

by P. DAVIDSON†, A. M. LEVELUT†, M. F. ACHARD‡ and F. HARDOUIN‡

† Laboratoire de Physique des Solides associé au CNRS Bat. 510 Université Paris XI 91405 Orsay Cedex, France

‡ Centre de Recherche Paul Pascal, Université de Bordeaux I, 33405 Talence, France

(*Received 29 July 1988; accepted 16 December 1988*)

A series of four mesomorphic side chain polysiloxanes has been studied by X-ray diffraction. They all exhibit smectic A phases around 100–150°C and smectic B or crystalline phases at room temperature. Oriented diffraction patterns in the smectic A phase display up to five orders of reflection on the smectic layers. The projection of the electron density profile along the normal to the layers has been derived by measuring the intensities of the different orders. This profile agrees well with the molecular features as measured from Dreiding stereomodels. The backbones are confined in a layer of width 6 ± 2 Å along the director. In some cases, the backbones are sufficiently confined to present an electron density maximum comparable to that of the mesogenic cores. Then, a period $d/2$ appears in the electron density profile, and therefore the second order reflection becomes stronger than the first.

1. Introduction

One of the main questions raised by mesomorphic side chain polymers as compared to their low molecular weight counterparts is how the backbones organize themselves in the different mesophases. *A priori*, X-ray diffraction on polyacrylates and polymethacrylates does not provide precise information on the backbones because of the poor electron density contrast between the backbones and the other aliphatic parts of the molecule such as the spacers or the aliphatic end groups if they exist. Small angle neutron scattering on partially deuteriated polymers is then a powerful method to obtain such information [1].

However, some mesomorphic side-chain polymers possess backbones with a larger electron density. Gudkov [2] has investigated a mesomorphic polymethacryloyl-ω-aminolaurate by X-ray diffraction in the partial bilayer S_{A_d} phase. By inverse Fourier transform, he found the backbones to be localized in a sublayer roughly 10 Å wide along the director. Mesomorphic side chain polysiloxanes also possess backbones with a large electron density because of the silicon atoms. Indeed some of them display a large number of Bragg reflections on the smectic layers as compared to other polymers such as polyacrylates or polymethacrylates. We therefore studied, by X-ray diffraction, four polymers belonging to the series synthesized and

0267–8292/89 $3.00

Table 1. Phase transition temperatures of the polymers $P_{3,4}$, $P_{4,4}$, $P_{3,8}$, and $P_{5,8}$. T_g: glass temperature T_{CS_A}: melting temperature T_{S_AI}: clearing point.

		$T_{S_BS_A}$/°C	
	T_g/°C	CS_A T/°C	S_AI T/°C
$P_{3,4}$	21 C	63 S_A	181 I
$P_{4,4}$	31 C	75 S_A	141 I
$P_{3,8}$	S_B	75 S_A	153 I
$P_{5,8}$	S_B	95 S_A	165 I

characterized by Mauzac *et al.* [3]; these correspond to the formula:

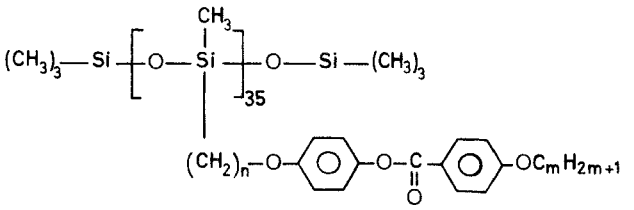

Among these polymers, denoted by $P_{n,m}$, we have studied the polymers $P_{3,4}$, $P_{4,4}$, $P_{3,8}$ and $P_{5,8}$ which were all reported to present usual S_A phases for which the layer thickness is close to the length of the side chain. Their mesomorphic properties are listed in table 1.

2. Experimental

Well aligned samples were produced [4] by slowly cooling (≈ 5°C/h) the samples from the isotropic phase into the smectic A phase in a magnetic field of 1·7 T. Switching off the field at room temperature or at a few degrees below T_{S_AI} does not alter the alignment (at least for a few days in the latter case).

We have obtained oriented diffraction patterns of each polymer in the following way [4]. The sample contained in a Lindemann capillary of 1·5 mm diameter was mounted in an oven heated by an air stream. The temperature of the sample was kept constant to within $\pm$ 1°C. The oven was placed between the poles of an electromagnet in an evacuated camera so as to eliminate air diffusion. A monochromatic (λCuK_α = 1·541 Å) point focused X-ray beam was obtained by reflection on a doubly bent pyrolytic graphite monochromator. The diffracted X-rays were collected on a cylindrical film at a distance, R, of 60 mm from the sample. In this geometry, we have cylindrical symmetry about the magnetic field direction.

Figure 1 shows the diffraction pattern of polymer $P_{5,8}$, in the S_A phase; polymers $P_{3,4}$, $P_{4,4}$ and $P_{3,8}$ give similar patterns. At small angles and along the magnetic field direction (the meridian, Oz), we find a series of equidistant Bragg spots (*a*): these are the smectic layer reflections which are resolution limited. Five orders of reflection can be seen in figure 1. At wide angles and in the directions perpendicular to the magnetic field (the equator, Ox and Oy), there are diffuse crescents (*b*) which show that the mesogenic cores are aligned along the meridian and that the layers are liquid-like. This pattern is therefore quite typical of a smectic A phase. Moreover, table 2 [3] shows that the smectic period d and the length l of the side chains are comparable: $d \approx 1$

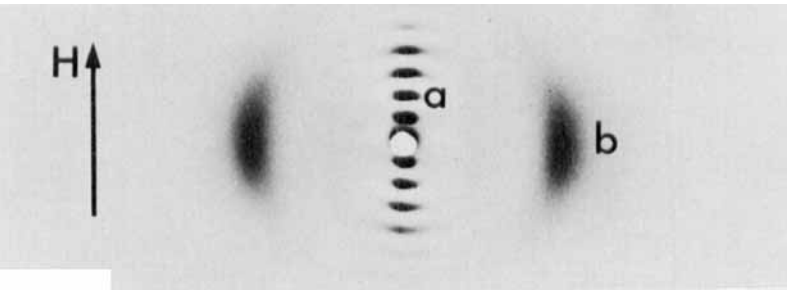

Figure 1. X-ray diffraction pattern of the polymer $P_{5,8}$ in its S_A phase (100°C) obtained using a point focusing X-ray beam of wavelength $\lambda CuK_\alpha = 1{\cdot}541$ Å. H is the magnetic field direction. (a) Bragg reflections and (*b*) wide angle diffuse crescents.

Table 2. Smectic periods *d* and lengths *l* of the side chains in the most extended configuration with SASM stereomodels.

	d/Å	*l*/Å
$P_{3,4}$	25·5	26
$P_{4,4}$	28	28
$P_{3,8}$	28·5	32
$P_{5,8}$	32	34·5

for $P_{3,4}$ and $P_{4,4}$; $d \approx 0{\cdot}951$ for $P_{3,8}$ and $P_{5,8}$. By length of the side chain, we mean the length of the pendant group added to the length of the $Si–CH_3$ group of the backbone on which the side chain is grafted; *l* is measured in the most extended configuration using SASM stereomodels.

Overexposed photographs also show that a fair amount of the scattered intensity is localized in diffuse lines and diffuse spots. These elements are similar to those displayed by some of the mesomorphic side-chain polymethacrylates [4] and they are due to fluctuations around the mean smectic A structure. Here we are only interested in the mean structure as revealed by the intensities of the Bragg reflections and so these fluctuations will not be considered (they will be discussed in a later paper).

It is quite unusual to observe so many orders of reflection in the scattering pattern of a thermotropic smectic A phase. That so many orders are observed means that the projection of the electron density profile along the director cannot be described by the ideal model of a single sinusoidal modulation [5] commonly employed for low molecular weight liquid crystals. This reflects the influence on the profile of the siloxane backbones. The intensities of the different Bragg reflections were measured in order to obtain more information on the electron density profile and on the localization of the siloxane backbones. Since the Bragg spots are resolution limited, we are only interested in the intensities of the reflections (and not in their profiles).

Samples were aligned by cooling in a magnetic field as described previously and were examined using a classical powder Guinier camera. Their diffraction patterns were recorded using CuK_α radiation obtained by reflection on a cylindrical quartz monochromator. The geometry of the experiment was the following: the sample contained in the Lindemann capillary rotates around its vertical axis. Then the director sweeps the horizontal plane which is the plane of diffusion. The horizontal X-ray beam, in the shape of a small vertical segment ($0{\cdot}1 \times 10\,mm^2$), is focused by

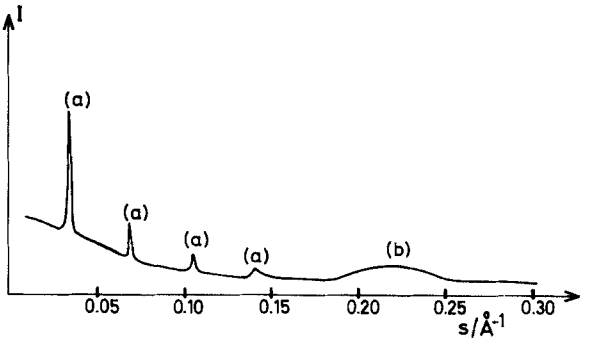

Figure 2. Microdensitometric profile of the powder pattern of an aligned sample of polymer $P_{3,8}$ in its S_A phase. (*a*) Bragg reflections, and (*b*) wide angle diffuse crescents. *I* is the intensity and *s* is the modulus of the scattering vector.

the monochromator onto the cylindrical film. The geometry is that of a rotating single crystal where the reciprocal nodes are only located on a single row. The samples were heated by an air stream and their temperature was held constant within ± 1°C. Several exposures were made so as to measure the strongest and the weakest reflections. Figure 2 shows an example of such powder patterns.

In our geometry, the Lorentz factor is

$$L(\theta) = \frac{1}{\sin 2\theta}$$

and the use of the (101) reflection on the quartz monochromator induces a polarization factor

$$P(\theta) = \frac{1 + \cos^2 2\alpha \cos^2 2\theta}{1 + \cos^2 2\alpha},$$

with $\alpha = 13°21'$. The experimental results have therefore been corrected for the combined Lorentz–polarization factor

$$\mathrm{LP}(\theta) = \frac{0{\cdot}556 + 0{\cdot}444 \cos^2 2\theta}{\sin 2\theta},$$

although the absorption corrections proved negligible. Since we do not measure the absolute scattering intensities, we present all the results as ratios a_n/a_1 of the amplitude of the nth order of reflection to the amplitude of the first (see table 3).

Table 3. Experimental amplitudes of diffraction of the different orders of reflection on the smectic layers. These amplitudes corrected for the Lorentz–polarization factor are normalized so that the amplitudes of the first order is one. The last two columns correspond to the smectic B phases at room temperature of polymers $P_{3,8}$ and $P_{5,8}$.

	$P_{3,4}$	$P_{4,4}$	$P_{3,8}$	$P_{5,8}$	$(P_{3,8})_B$	$(P_{5,8})_B$
a_1	1	1	1	1	1	1
a_2	1·60	1·55	0·75	0·85	0·60	0·80
a_3	1·50	0·70	0·60	0·75	0·60	0·80
a_4	0·80	0	0·55	0·60	0·75	0·80
a_5	0	0	0	0·30	0	0·60

3. Determination of the electron density profile along the director

We denote the projection of the electron density profile along the director $\varrho(z)$ (see figure 3). We take the origin of the z axis in the middle of the region of backbones and assume that we have as many mesogenic cores pointing in the $+z$ direction as in the $-z$ direction. Then $\varrho(z)$ must be symmetric, $\varrho(-z) = \varrho(z)$ and since it is a periodic function of period d, it can be expressed as a Fourier series where only the cosine terms are relevant [2];

$$\varrho(z) = \varrho_0 + 2\sum_{n=1}^{\infty} A_n \cos\left(n2\pi\frac{z}{d}\right).$$

Since we do not measure ϱ_0 but only the fluctuations around ϱ_0, we write $\varrho(z)$ to represent only the fluctuations

$$\varrho(z) = \sum_{n=1}^{\infty} a_n \cos\left(n2\pi\frac{z}{d}\right).$$

The coefficients a_n are real but may be positive or negative.

The intensity of the nth order reflection is directly proportional to $|a_n|^2$ where $|a_n|$ is the modulus of a_n. The phase problem reduces to choosing the right combination of signs for the coefficients a_n. We call, for example, $\varrho_{-++-}(z)$ the combination where a_1 and a_4 are chosen negative while a_2 and a_3 are chosen positive. From figure 3 we can obtain an idea of what physically acceptable solutions for $\varrho(z)$ should look like. We can compute the average value, ϱ_0, of the projection, $\varrho(z)$, of the electron density along the director by dividing the total number of electrons of the polymer repeat unit by the dimension, d, of the unit cell: $\varrho_0 \approx 8{\cdot}0 \pm 0{\cdot}5 e^-/Å$ or more precisely:

$$P_{3,4}: \varrho_0 = 8{\cdot}2 \pm 0{\cdot}1 e^-/Å; \quad P_{4,4}: \varrho_0 = 7{\cdot}7 \pm 0{\cdot}1 e^-/Å;$$

$$P_{3,8}: \varrho_0 = 8{\cdot}4 \pm 0{\cdot}1 e^-/Å; \quad P_{5,8}: \varrho_0 = 8{\cdot}0 \pm 0{\cdot}1 e^-/Å.$$

Then the electron density of the mesogenic core can be evaluated by dividing its number of electrons by its size: $\varrho_{core} \approx 9{\cdot}5 \pm 0{\cdot}5 e^-/Å$ (this is only a crude estimate

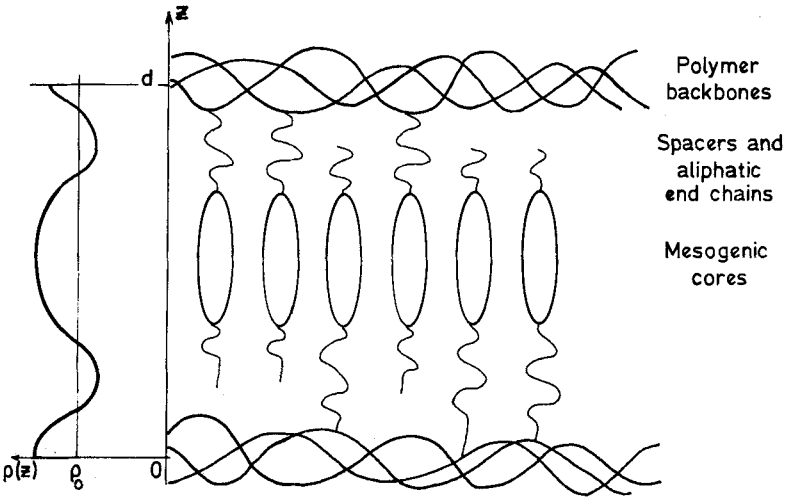

Figure 3. Schematic representation of the structure of the S_A phase of polymers $P_{3,4}$, $P_{4,4}$, $P_{3,8}$ and $P_{5,8}$.

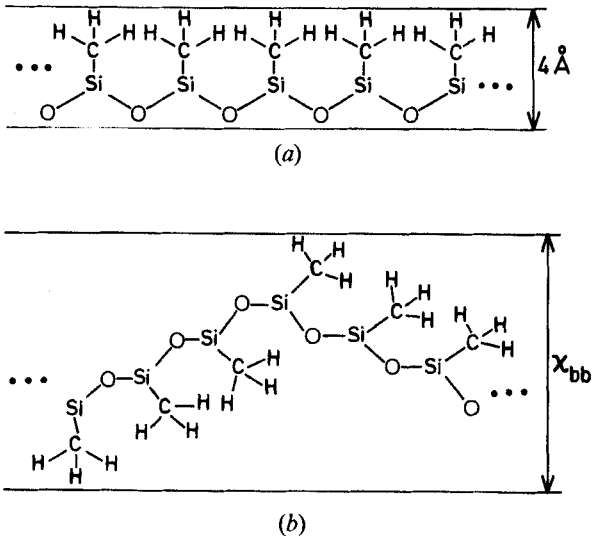

(*a*)

(*b*)

Figure 4. Two different configurations of the backbones, (*a*) completely confined in a width 4 Å, and (*b*) confined in a width x_{bb}. In this figure, the side chains have been omitted for the sake of clarity.

because it neglects the translational fluctuations which spread out this maximum of the electron density).

The electron density of the aliphatic parts, ϱ_{al}, is evaluated as follows. The density of some $P_{n,m}$ polymers has already been measured [6] from which a classical value of $V_{CH_2} \approx 30\,Å^3$ per methylene group was obtained. The following molecular areas were then derived, $S \approx 22\,Å^2$ for $P_{5,4}$ and $23{\cdot}5\,Å^2$ for $P_{5,8}$. Dividing V_{CH_2} by S gives us an average value of the width l_{CH_2} along Oz of a CH_2 link. Now, since there are eight electrons per CH_2 (9 for the CH_3 end group), ϱ_{al} is approximately equal to $8/l_{CH_2}\,e^-/Å$, that is $5{\cdot}95 \pm 0{\cdot}30\,e^-/Å$ for $P_{3,4}$ and $P_{4,4}$ and $6{\cdot}35 \pm 0{\cdot}30\,e^-/Å$ for $P_{3,8}$ and $P_{5,8}$.

The electron density of the backbone ϱ_{bb} depends on its degree of confinement; the more the backbone is confined, the larger is its electron density. We can estimate ϱ_{bb} approximately in a simple way: first consider a completely confined backbone (see figure 4 (*a*)), its width is approximately 4 Å, then its electron density is $33{\cdot}6/4 = 8{\cdot}4\,e^-/Å$. This density is larger than that of the aliphatic parts by $8{\cdot}4 - \varrho_{al} \approx 2{\cdot}4\,e^-/Å$. Now if the backbone is confined within a distance x_{bb} (see figure 4 (*b*)), then this excess of density is spread over x_{bb} and we have

$$\varrho_{bb} = \varrho_{al} + \frac{2{\cdot}4 \times 4}{x_{bb}}$$

This means that $\varrho(z)$ should have a second maximum due to the siloxane backbones. The larger this maximum, the smaller its width.

Though our estimates of the different electron densities are very crude, we should only accept the solutions which present a wide central maximum for $z = d/2$ caused by the mesogenic cores and another maximum for $z = 0$ caused by the siloxane backbones. The case of polymer $P_{4,4}$ is the simplest since we only observe three orders of reflection; figures 5 (*a–h*) show all of the combinations of signs possible. Figures 5 (*a–d*) are solutions which present a strong central minimum and are not physically acceptable. Figures 5 (*e–h*) are solutions which all present maxima for $z = 0$ and $z = d/2$.

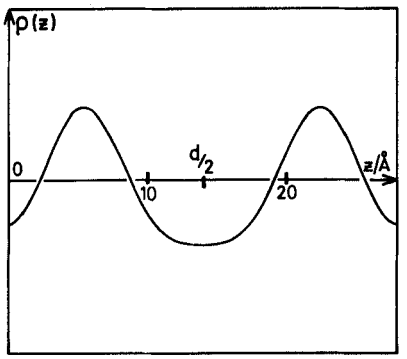

(*a*)

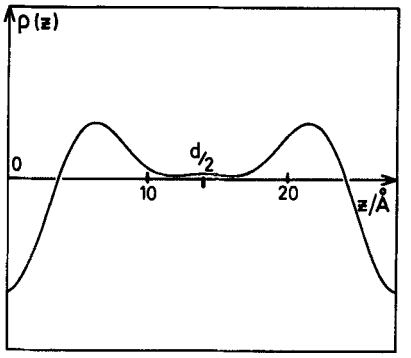

(*b*)

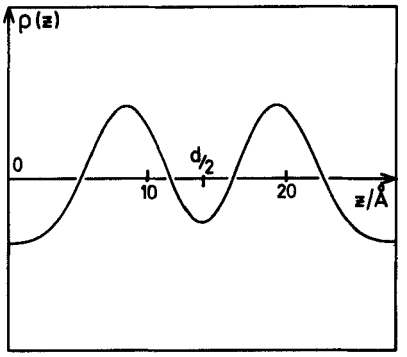

(*c*)

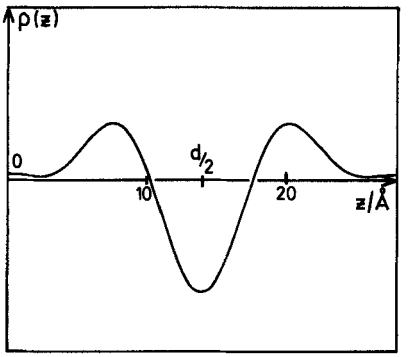

(*d*)

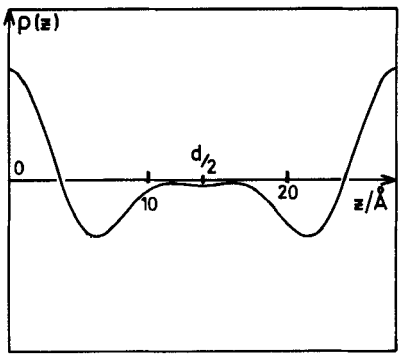

(*e*)

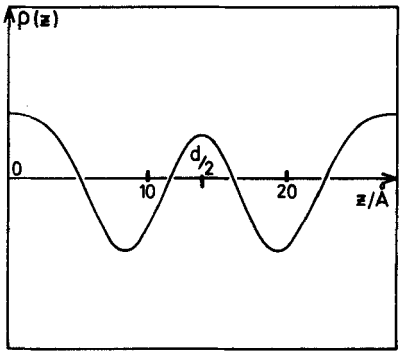

(*f*)

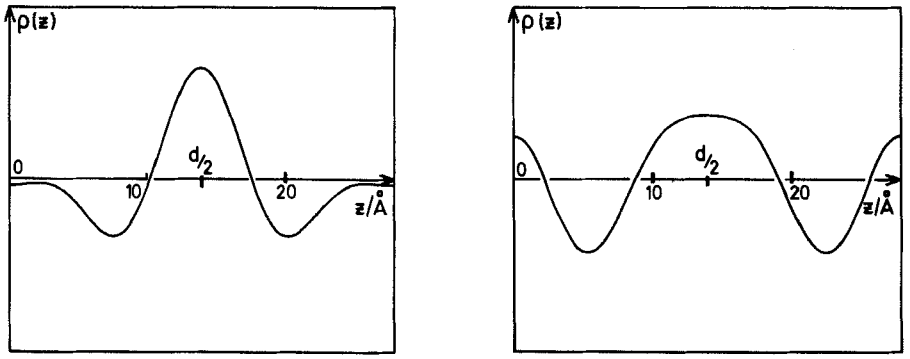

(*g*) (*h*)

Figure 5. (*a*)–(*h*) Polymer $P_{4,4}$. Different projections of the electron density profile which correspond to all of the different sign combinations of the a_n coefficients. (*a*) $\varrho_{+--}(z)$, (*b*) $\varrho_{---}(z)$, (*c*) $\varrho_{--+}(z)$, (*d*) $\varrho_{+-+}(z)$, (*e*) $\varrho_{+++}(z)$, (*f*) $\varrho_{++-}(z)$, (*g*) $\varrho_{-+-}(z)$, (*h*) $\varrho_{-++}(z)$.

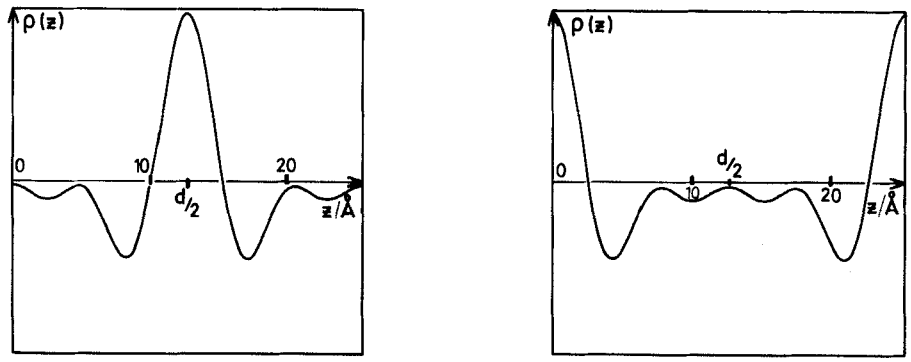

(*a*) (*b*)

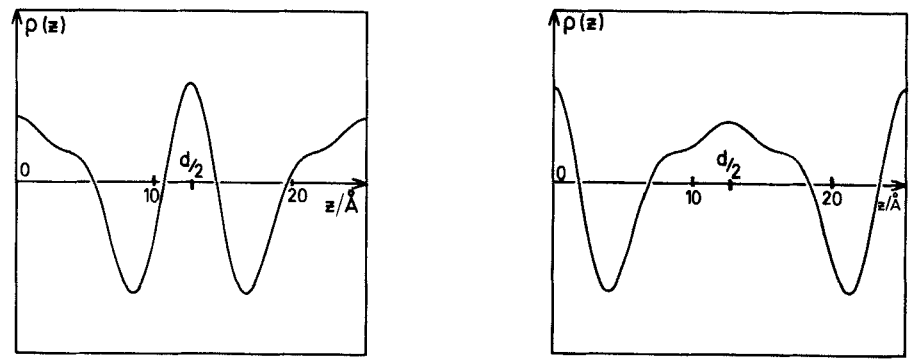

(*c*) (*d*)

Figure 6. (*a*)–(*d*) Polymer $P_{3,4}$. The four electron density profiles which display maxima for $z = 0$ and $z = d/2$. (*a*) $\varrho_{-+-+}(z)$, (*b*) $\varrho_{++++}(z)$, (*c*) $\varrho_{++-+}(z)$, (*d*) $\varrho_{-+++}(z)$.

At this point, we may use the parameter called r by Etherington *et al.* [7] and defined by

$$r = \frac{\varrho_0 - \varrho_{al}}{\varrho_{core} - \varrho_{al}}.$$

This parameter helps us to appreciate which solutions give a proper electron density to the core compared with that of the aliphatic parts of the molecule. However, r is difficult to evaluate precisely because of the poor accuracy on the electron densities. For polymer $P_{4,4}$ we have $r = 0{\cdot}50 \pm 0{\cdot}15$. For each solution, we may calculate r; thus for figure 5 (*e*) $r \approx 1$; for figure 5 (*f*) $r = 0{\cdot}62$; for figure 5 (*g*) $r = 0{\cdot}33$; and for figure 5 (*h*): $r = 0{\cdot}54$. Thus the solutions in figure 5 (*e*) and (*g*) should be rejected, that in figure 5 (*h*) falls very close to the calculated value but the solution in figure 5 (*f*) cannot be rejected on this basis. However figure 5 (*f*) gives a maximum both larger and wider to the region of backbones than that of the mesogenic cores; this is not very likely and therefore we discard this solution. Then, we are left with only one possible solution namely that in figure 5 (*h*).

The case of polymer $P_{3,4}$ is more complicated since it exhibits four orders of reflection and then there are sixteen possible combinations of signs. Among them, only four have maxima both for $z = 0$ and $z = d/2$; they are shown in figures 6(*a*)–(*d*). The first two solutions must be discarded because they give a ratio r incompatible with the calculated value of $0{\cdot}60 \pm 0{\cdot}15$ (see figure 6 (*a*): $r = 0{\cdot}31$ and figure 6 (*b*): $r \approx 1$). Solutions ϱ_{-+++} and ϱ_{++-+} represented in figures 6 (*c*) and (*d*) both give acceptable r values (for figure 6 (*c*): $r = 0{\cdot}53$ and figure 6 (*d*): $r = 0{\cdot}64$). Actually we have $\varrho_{-+++}(z + d/2) = \varrho_{++-+}(z)$ which means that both profiles are similar but we have to decide which maximum corresponds to the cores and which maximum

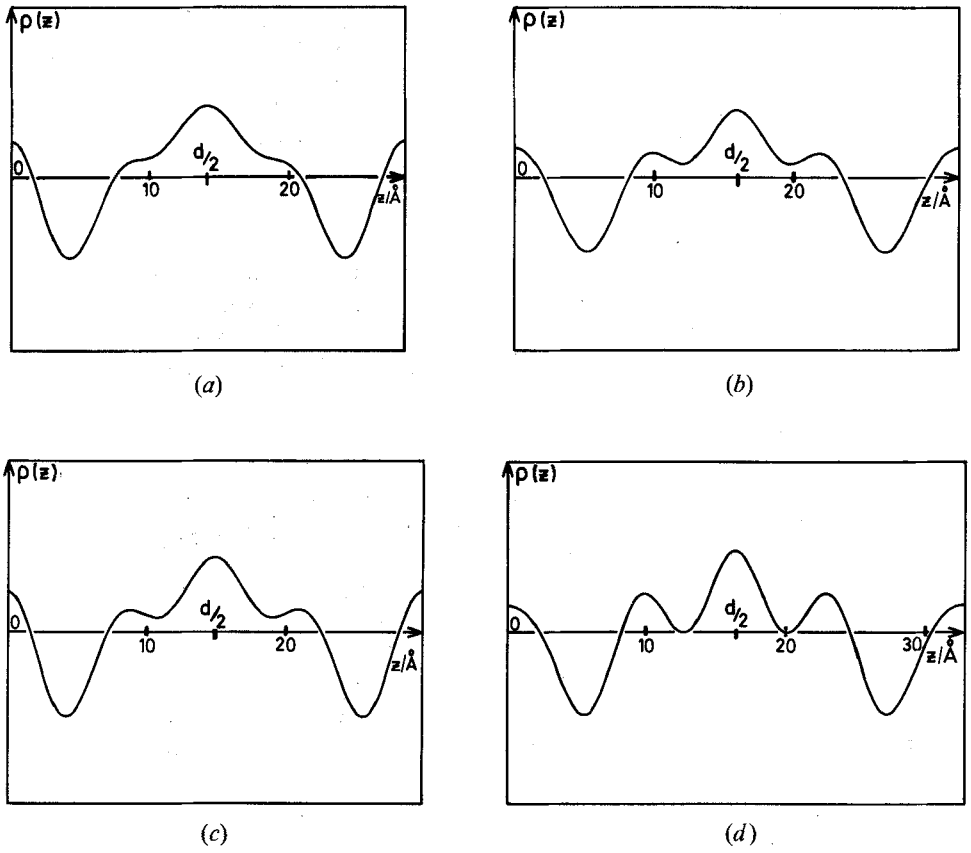

Figure 7. (*a*)–(*d*) Polymers $P_{3,8}$ and $P_{5,8}$. Possible electron density profiles $\varrho_{-+++}(z)$ for each polymer. (*a*) S_A phase of $P_{3,8}$, (*b*) S_A phase of $P_{5,8}$, (*c*) S_B phase of $P_{3,8}$, (*d*) S_B phase of $P_{5,8}$.

corresponds to the backbones. We would rather favour solution $\varrho_{-+++}(z)$ (see figure 6 (*d*)) since it attributes the wider maximum to the region of mesogenic cores (this situation is similar to that of polymer $P_{4,4}$).

We now consider polymers $P_{3,8}$ and $P_{5,8}$. Figures 7 (*a*) and (*b*) show the solutions which seem to us closest to a physically acceptable solution (on the basis of the two previously defined criteria, namely the existence of two maxima for $z = 0$ and $z = d/2$ and acceptable values for the ratios r. For figure 7 (*a*): $\varrho_{-+++}(z)$, $r = 0{\cdot}53$, calculated value $r = 0{\cdot}65 \pm 0{\cdot}2$; figure 7 (*b*): $\varrho_{-+++-}(z)$, $r = 0{\cdot}52$, calculated value $r = 0{\cdot}55 \pm 0{\cdot}2$; figure 7 (*c*): $\varrho_{-+++}(z)$, $r = 0{\cdot}53$, calculated value $r = 0{\cdot}55 \pm 0{\cdot}2$; figure 7 (*d*): $\varrho_{-+++-}(z)$, $r = 0{\cdot}50$, calculated value $r = 0{\cdot}45 \pm 0{\cdot}2$). Figures 7 (*c*) and (*d*) show these solutions in the smectic B phase. In the next section, we compare the different electron density profiles which correspond to those of our polymers.

4. Discussion

As expected, the possible electron density profiles for all the polymers look similar: they exhibit a large central maximum due to the mesogenic cores, a secondary maximum caused by the backbones and two equivalent minima which correspond to the regions of mixed spacers and aliphatic end chains. In addition, the sign combinations chosen for the different polymers are the same. This could not be predicted at once because the polymers differ by their periods d.

We now compare the electron density profile of polymer $P_{4,4}$ (see figure 5 (*h*)) with that of polymer $P_{3,4}$ (see figure 6 (*d*)). We can see in figure 6 (*d*) that the region of the backbones is about 5 Å wide along the director. For polymer $P_{4,4}$, the width of this region is approximately 6 Å (see figure 5 (*h*)). These values show that the backbones are strongly confined between the layers in two dimensions and consequently their apparent electron density becomes comparable to that of the mesogenic cores. This induces a period, $d/2$, in the electron density profile and explains why the amplitude of the second order reflection is much larger than that of the first for polymers $P_{3,4}$ and $P_{4,4}$. (The same type of inversion has been observed by Gudkov [2] in a series of mesomorphic polymethacryloyl-ω-aminolaurates which he explained in a similar manner). We have observed another type of intensity inversion in a series of cyano-substituted side chain polyacrylates [8]. These polymers have a S_{A_d} phase ($d \approx 1{\cdot}8l$) for which the 3rd order reflection is stronger than the 1st and the 2nd. This effect is explained by taking into account the influence of the backbones on the electron density profile. However comparing these two series of polymers, we can see that the backbones are more confined for the case of the polysiloxanes than for the polyacrylates. We explain this effect by recalling that in the S_{A_d} phase of the polyacrylates, the backbones delocalize themselves by squeezing the flexible spacers. The spacers are indeed longer in the polyacrylate series than in the other. Moreover the compactness of a S_{A_d} phase is smaller than that of a S_{A_1} phase and this should help the backbones to expand in the former case.

Now, let us compare polymers $P_{3,8}$ and $P_{5,8}$ with polymers $P_{3,4}$ and $P_{4,4}$. We notice that the secondary maximum due to the backbones is much smaller than the central maximum for polymers $P_{3,8}$ and $P_{5,8}$. Indeed the data in table 3 shows that the first order reflection is stronger than the second for these two polymers. The presence of long aliphatic tails may help the backbones to spread out, thus decreasing their electron density. In the same way, it seems that the backbones are more confined for polymer $P_{3,4}$ than for polymer $P_{4,4}$ (see figures 5 (*h*) and 6 (*d*)). Thus, in this series,

adding aliphatic parts to the molecule helps the backbones to resist the confinement imposed by the mesogenic cores.

We also notice that for both polymers $P_{3,8}$ and $P_{5,8}$, and to a lesser extent for polymer $P_{3,4}$, the electron density profiles present some details in the region of the central maximum. These details are more obvious in the smectic B phase (see figures 7(*c*) and (*d*)) and may correspond either to the molecular structure of the mesogenic cores or to positional shifts of the mesogenic cores along the director.

5. Conclusion

We have obtained X-ray diffraction patterns for oriented smectic A phase for all four polymers studied. The large number of reflections from the smectic layers has prompted us to derive the projection of the electron density profile along the normal to the layers. We have measured the intensities of the different orders of reflection on the smectic layers and generated all of the sign combinations for the different harmonics. Among these, only a few possible solutions can be recognized as physically acceptable. This method is particularly efficient here because several polymers of the same series can be compared. For some cases, two different mesophases S_A and S_B of the same polymer can also be compared. The sign combinations chosen for all the polymers studied are the same in both the S_A and the S_B phases.

The density profiles which we obtained are in agreement with a simple image of the organization of the phase. The smectic layer is divided into sublayers consisting of the mesogenic cores, the spacers and the aliphatic tails respectively; the backbones are strongly squeezed between the other sublayers. The width of the backbone sublayer varies from approximately 5 Å for $P_{3,4}$ to 7 Å for $P_{5,8}$. For the polymers $P_{3,4}$ and $P_{4,4}$, the backbones seem to be squeezed sufficiently to induce an intensity inversion between the first and the second orders reflection. By considering the various elastic properties of the backbones and the spacers, it might be possible to predict theoretically the width in which the backbones are confined.

The authors would like to thank Drs. M. Mauzac and H. Richard for kindly providing the samples, Dr. G. Sigaud for stimulating discussions and Dr. A. Braslau for reviewing the English manuscript.

References

[1] Keller, P., Carvalho, B., Cotton, J. P., Lambert, M., Moussa, F., and Pepy, G., 1985, *J. Phys. Lett., Paris*, **46**, L1065.
[2] Gudkov, V. A., 1984, *Sov. Phys. Crystallogr.*, **29**, 316.
[3] Mauzac, M., Hardouin, F., Richard, H., Achard, M. F., Sigaud, G., and Gasparoux, H., 1986, *Eur. Polym. J*, **22**, 137.
[4] Davidson, P., Keller, P., and Levelut, A. M., 1985, *J. Phys., Paris*, **46**, 939.
[5] De Gennes, P. G., 1974, *The Physics of Liquid Crystals* (Clarendon Press).
[6] Achard, M. F., Hardouin, F., Sigaud, G., and Mauzac, M., 1986, *Liq. Crystals*, **1**, 203.
[7] Etherington, G., Langley, A. J., Leadbetter, A. J., and Wang, X. J., 1988, *Liq. Crystals*, **3**, 155.
[8] Davidson, P., and Strzelecki, L., 1988, *Liq. Crystals*, **3**, 1583.